

Superstrate-Based Low Observable Cavity-Backed Archimedean Spiral Antenna (2–18 GHz) for Electronic Warfare Applications

Christy A. Prasad, Abhina A. Manoj, Shrikrishan Baghel,
Konidala S. Venu, Vineetha Joy*, and Hema Singh

Centre for Electromagnetics, CSIR-National Aerospace Laboratories, Kodihalli, Bangalore 560017, India

ABSTRACT: A superstrate comprising a dielectric and metasurface pattern, placed at an optimum height from the antenna surface, can facilitate radar cross section (RCS) reduction of the antenna. An optimally designed superstrate will not degrade the radiation performance of the antenna. In this paper, a novel design of low RCS superstrate-based right-handed circularly polarized (RHCP) cavity-backed Archimedean spiral (CBAS) antenna has been presented. The superstrate consists of a resistive sheet-based metasurface pattern on the top layer and a metallic pattern on the bottom surface of a dielectric substrate. It is shown that the proposed thin (0.82 mm) superstrate placed at an optimal height of 19.2 mm from the antenna surface resulted in the RCS reduction of 6–8 dBsm over the operating frequency range (2–18 GHz), without any degradation in VSWR (< 2.1), gain (> 3 dBi), and axial ratio (< 3 dB). Such a low observable, cost-effective, and efficient spiral antenna without any payload constraints can be a preferred choice for electronic warfare applications in aerospace platforms.

1. INTRODUCTION

Electronic warfare (EW) systems constitute various ranges of state-of-the-art technologies and techniques such as radar systems, communication systems, signal processing, and data processing. An important aspect of EW is the development of Fire Control Radar (FCR) and radar warning receiver (RWR), a type of radar system used to track, identify, elude targets, and guide weapons systems. Wideband capability is an important feature in electronic warfare scenarios in order to counteract electronic threats of different frequencies. A cavity-backed Archimedean spiral (CBAS) antenna is a radio frequency (RF) antenna used for direction-finding and EW applications [1, 2] owing to its wideband characteristics, symmetric radiation, and high directivity.

When designing a stealth platform, antennas mounted on the surface often contribute significantly to the overall radar cross section (RCS). To minimize RCS, strategies beyond shaping and the use of radar absorbing materials and structures are employed. One effective approach is to make the antennas conformal. Further RCS reduction can be achieved through advanced design techniques, such as incorporating a defected ground plane, integrating microwave absorbers (MAs), and using an optimized superstrate layer. The antenna performance, especially in terms of RCS, is difficult to control. Antenna, being a radiating device, is designed to have maximum gain and low voltage-standing-wave-ratio (VSWR) in its operating frequency range. Any change in the structure towards reducing the scattering can adversely affect its radiation performance. One of the most efficient techniques to handle such constraint is to use optimally designed superstrate over the antenna structure.

A superstrate typically consists of a dielectric layer integrated with a metasurface-based pattern, which can be realized using either metallic or resistive materials. Its performance depends on factors such as the pattern geometry, properties of the dielectric substrate, and the configuration of the layers (whether they function as partially reflecting or absorbing surfaces). The superstrate is positioned at an optimal distance above the antenna to preserve its radiation characteristics while simultaneously reducing the structural RCS [3]. Initially, superstrates served mainly as protective layers for low-profile antennas operating in harsh environmental conditions. However, with carefully optimized design parameters, they have evolved to enhance antenna performance significantly, particularly by improving gain and broadening the operational bandwidth [4–8].

Superstrates have been made for low-profile antenna especially microstrip patch antenna and slot antenna but not for actual antennas used in aerospace platforms. The challenge is mainly the performance bandwidth of the superstrate in maintaining radiation characteristics [3–8]. The difficulty in superstrate design increases when scattering performance of the antenna is also considered [9–14]. The antenna RCS is required to be reduced but with maintained gain and VSWR in the operating frequency range.

Archimedean spiral antenna is considered a good choice for ultra-wideband (UWB) applications since it is a broadband and frequency-independent antenna with high efficiency and compact form factor. One of the important features of a CBAS antenna is its unidirectional radiation pattern. In this paper, a low-RCS wideband right-handed circularly polarized CBAS antenna with a three-layered superstrate is presented. The operating frequency of the proposed antenna is 2–18 GHz, well

* Corresponding author: Vineetha Joy (vineethajoy@nal.res.in).

suitable for EW applications. The antenna and superstrate have been designed and developed using commercially available substrates and resistive/metallic materials. The superstrate is a thin (0.82 mm thickness) structure with minimal weight addition to the antenna system. It consists of a resistive sheet-based metasurface pattern on the top layer and a metallic pattern on the bottom surface of the dielectric substrate. The designed and developed superstrate-based CBAS antenna demonstrates 6–8 dB RCS reduction over 2–18 GHz without affecting its VSWR, axial ratio, and antenna gain. It is shown that measured results corroborate the capability of the designed antenna. The presented cost-effective wideband low-RCS antenna is in line with the requirement of low observable antennas for stealth platforms.

2. EM DESIGN OF SUPERSTRATE-BASED CBAS ANTENNA

Here, a low-profile spiral antenna has been designed by etching metal in a spiral pattern on a dielectric substrate. The antenna is fed at the center by an internal balun (Fig. 1). Such a spiral antenna radiates in both the broadside directions. In order to have unidirectional radiation (in the forward direction) in a spiral antenna, a metal-backed lossy cavity is added behind the antenna. This arrangement helps in the absorption of back radiation from the spiral antenna and also reflections from the ground plane.

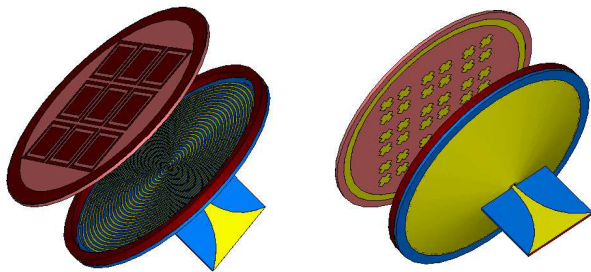


FIGURE 1. CBAS antenna with superstrate (V5).

An appropriate design of the cavity and optimum usage of an absorber helps in reducing the reflections and hence VSWR and the axial ratio of the antenna. Further, in order to achieve large operational bandwidth, the length of the spiral is increased by introducing a slow wave spiral structure of sinusoidal profile, thereby increasing the circumference of the antenna. This meandering in the spiral increases the electrical length and hence the bandwidth of the antenna. Further, the grounded absorber strip has been placed above the spiral section. The design parameters are listed in Table 1.

A superstrate consisting of three layers has been designed using commercially available substrates, resistive sheets, and metallic cladding. The top layer of the superstrate consists of metasurface-based unit cells, placed in an identified geometric pattern. This resistive sheet-based patterned layer on dielectric substrate RO4835 acts as a partially absorbing surface (PAS).

Typically, periodic patches and slots are incorporated into the metasurface unit cell to disrupt the uniform flow of surface currents, thereby enhancing its scattering properties. On

TABLE 1. Design parameters of cavity-backed Archimedean spiral antenna.

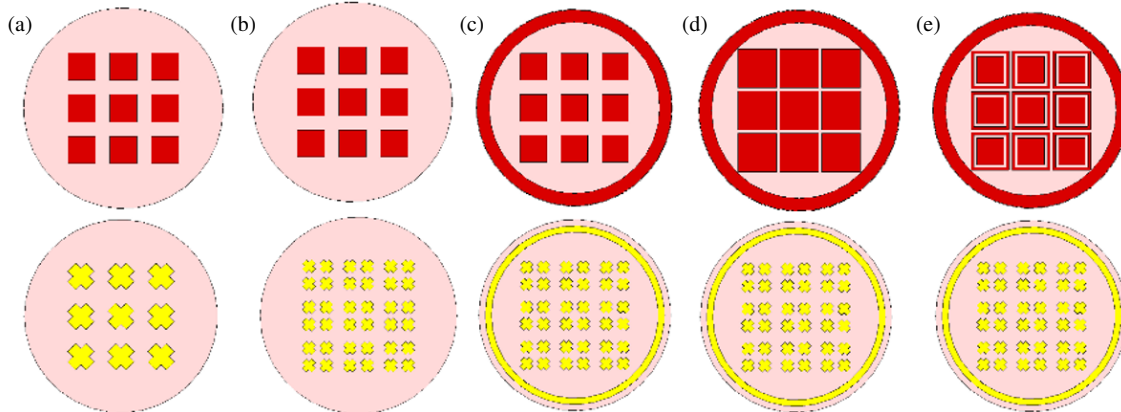
Parameter	Dimension
Thickness of substrate	0.787 mm
Length of balun	25 mm
Width of balun	20 mm
Width of signal trace unbalanced port	10.04 mm
Width of microstrip	0.5 mm
Gap between coils	0.5 mm
Diameter of spiral section	60.4 mm
No. of turns in each coil	13
Height of cavity	7.3 mm
Thickness of absorber strip	2 mm
Width of absorber strip	2.2 mm
Inner radius of absorber strip	28 mm
Thickness of metal used in cavity	0.5 mm

the underside of the substrate, metallic patch patterns are implemented to form a partially reflecting surface (PRS), which contributes to increased antenna gain [3]. However, the presence of these metallic patches in the superstrate can lead to enhanced backside radiation because of surface waves in the periodic structure, potentially reducing the overall antenna efficiency. To mitigate this problem, various techniques such as adding corrugations, metal strips, or vias on the surface have been reported in the literature. In the present design, the edge of a circular metallic cavity fulfills this role effectively. The comparison of the presented work with those reported in the open domain has been tabulated in Table 2. In this paper, metasurface elements are selected in view of the desirable bandwidth. The designed superstrate (V5) consists of square resistive patches on the front side and inverted metallic crosses on the back side, as shown in Fig. 1. The design of metasurface elements on the two surfaces of the superstrate has evolved (Fig. 2) keeping gain, axial ratio, and RCS in mind. As we move from V1 to V5, both the top and bottom surfaces of the superstrate change. On the top surface (PAS), one additional resistive square loop is added to an optimized square patch. This change has introduced additional capacitive and inductive elements. This change has contributed to gain maintenance over the operating bandwidth of 2–18 GHz. Further, the additional resistive ring at the outer edge of upper surface contributed to the maintenance of AR < 3 dB. The bottom surface (PRS) of V1 consists of metallic cross-shaped patches in order to achieve constructive interference between multiple reflections occurring between antenna surface and superstrate.

The addition of a metallic ring in the back pattern helps in maintaining axial ratio < 3 dB. It is evident from Fig. 3 that V2 shows gain improvement when the number of inverted crosses on the back pattern is increased along with optimized dimensions. However, the axial ratio is not < 3 dB beyond 16 GHz. The version V4 has bigger resistive patches in the front pattern and shows good RCS reduction over 8–12 GHz. However, the gain of the antenna has degraded. Thus, a resistive loop has been added in the square patch in V5. The strip width of the

TABLE 2. Comparison of the performance of the designed superstrate based CBAS antenna with other reported superstrate-based antennas.

Ref.	Antenna	Superstrate	Operating freq.range	Height above antenna	EM performance	RCS Reduction (RCSR)
[4]	EBG antenna	Square loop based FSS in superstrate	8-11 GHz	14.75 mm	BW increased by 5% Directivity increased by 6 dBi (70%)	-
[5]	Microstrip patch antenna	I-shaped metamaterial based superstrate	Multi-band (6.18 GHz, 9.65 GHz, 11.5 GHz)	7 mm	BW reduced by 3.9% (1 st fr) BW increased by 21% (2 nd fr) & 26% (3 rd fr) Gain increased by 74.28%	-
[6]	Microstrip patch antenna	Metamaterial-based superstrate	5-6 GHz	4.5 mm	Gain increased by 3 dBi	-
[7]	Slot antenna array	Liquid metal alloy-based superstrate	4.8-5.0GHz	5 mm	Gain maintained	Out-of-band RCSR of 10 dBsm (8-18 GHz)
[8]	Microstrip patch antenna	Graphene based frequency selective superstrate	5.04 to 5.21 GHz	15.4 mm	Gain increased by 2.4 dBi	In-band RCSR: 6 dBsm Out-of-band RCSR : 8 dBsm (2-14 GHz)
[9]	Fabry-Perot resonator antenna	Shared-aperture MM superstrate	7.3 GHz to 12.5 GHz	15.5 mm	Gain increased by 5-7 dBi	RCSR of 8 dBsm (av.) over 4-12 GHz
[10]	4×4 microstrip patch array	Resistively loaded FSS superstrate	8 GHz to 26 GHz	15 mm	Gain reduced by 2 dBi	RCSR of 10 dBsm (av.) over 8-26 GHz
This work	CBAS antenna	Resistive sheet based superstrate	2 GHz to 18 GHz	19.19 mm	Gain maintained	RCSR of 8 dBsm (av.) over 2-18 GHz

**FIGURE 2.** Evolution of EM design of superstrate for CBAS antenna. (a) V1, (b) V2, (c) V3, (d) V4, (e) V5.

loop and its spacing from the square patch have been optimized to achieve the best EM performance and good RCS reduction over 2–18 GHz, as shown in Fig. 3. As far as details of the superstrate design is concerned, the dimensions and positions of the unit cells in the front and bottom surfaces of the superstrate are shown in Fig. 4. The materials chosen for layers of the superstrate are:

Layer#1: Resistive sheet ($R_s = 377 \Omega/\text{sq.}$; $t_{res} = 0.018 \text{ mm}$)

Layer#2: RO4835 ($\epsilon_r = 3.48$; $\tan \delta = 0.0037$; $t_1 = 0.787 \text{ mm}$)

Layer#3: Copper annealed (thickness = 0.018 mm)

The total thickness of the superstrate = 0.823 mm.

The fabricated superstrate-based CBAS antenna is shown in Fig. 5. It is noted that while designing the superstrate-based CBAS antenna, utmost care has been taken to maintain the radiation characteristics, such as reflection coefficient, gain, VSWR, and axial ratio within the required limits.

3. EM PERFORMANCE AND RADAR CROSS SECTION OF SUPERSTRATE-BASED CBAS ANTENNA

The performance of CBAS antenna with a superstrate has been evaluated by placing the superstrate over the CBAS antenna at

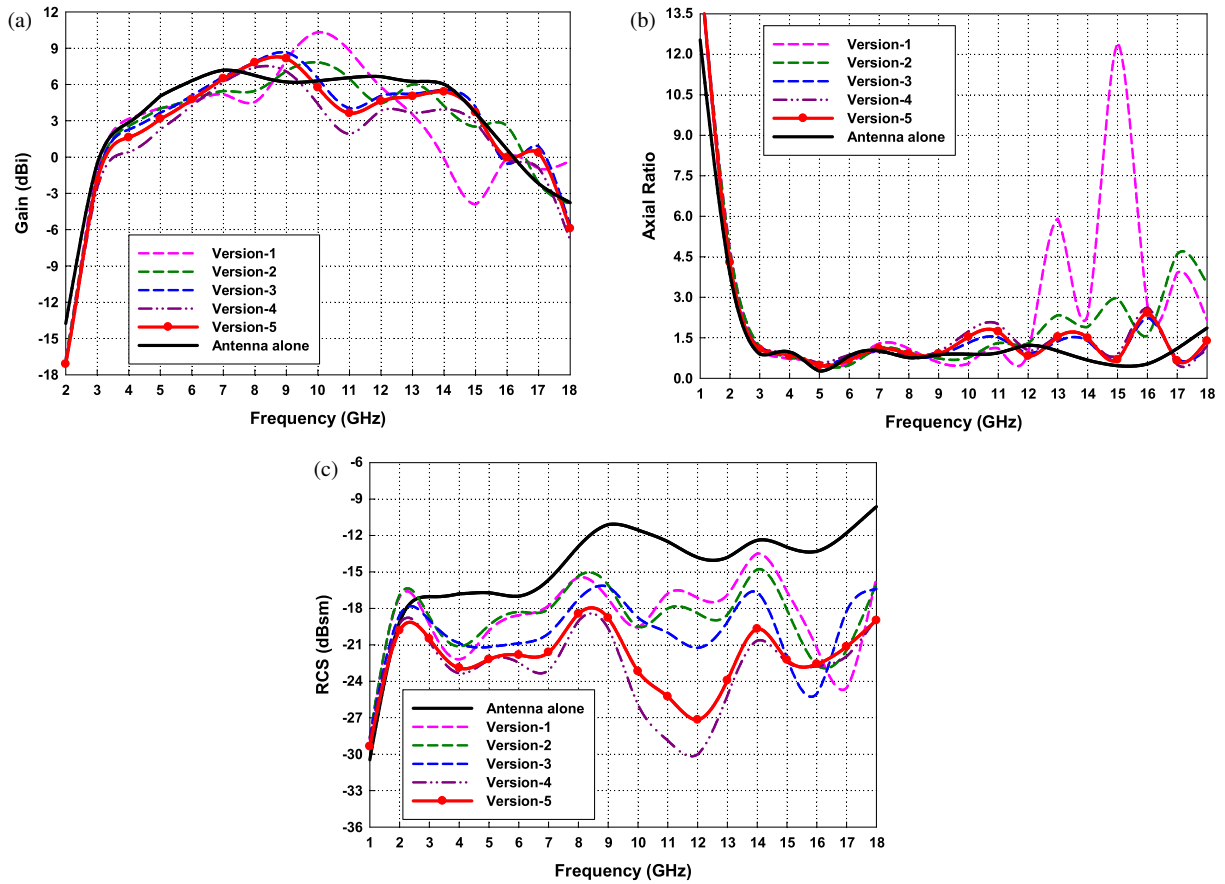


FIGURE 3. Simulated EM and RCS performance of CBAS antenna with different versions of superstrates.

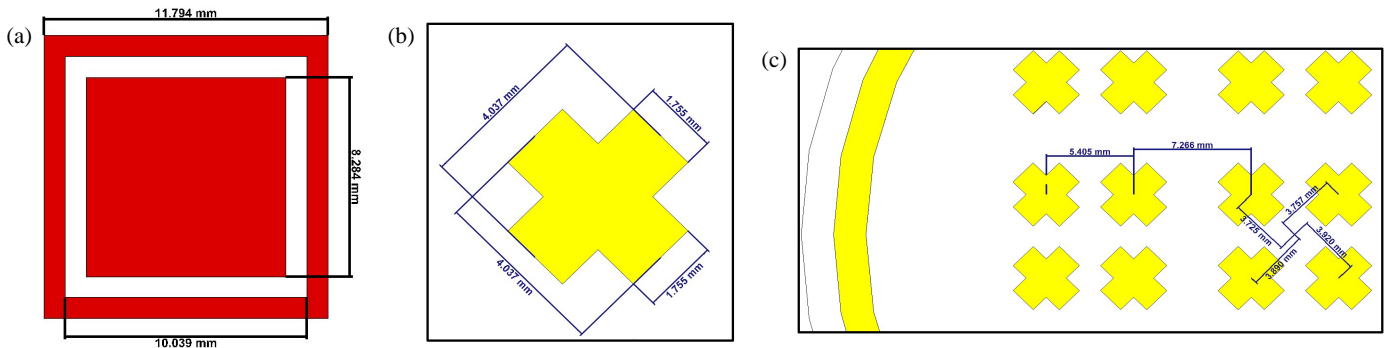


FIGURE 4. Zoomed view of designed unit cell. (a) Resistive unit cell on the top layer. (b) Metallic unit cell on the bottom layer. (c) Positions of the cross type unit cell.

a height of 19.20 mm. The measurement setups for EM performance and RCS measurements are shown in Fig. 6.

3.1. EM Performance

Figure 7 compares the simulated and measured EM performances in terms of VSWR, axial ratio, and the gain of the CBAS antenna with and without superstrate. It is evident that VSWR, axial ratio, and gain of the CBAS antenna remain well within the specified limits even after the addition of a superstrate above the antenna.

Since the CBAS antenna is right-handed circularly polarized, it is necessary to check its axial ratio performance for oblique angles of incidence as well. Fig. 8 presents the contour plot of the axial ratio of the CBAS antenna with/without superstrate. It is evident that the axial ratio of the antenna is maintained below 3 dB for normal as well as oblique angles of incidence. The simulated and measured radiation patterns of the CBAS antenna with/without a superstrate at 10 GHz are shown in Fig. 9 and Fig. 10, respectively. It is evident that the radiation pattern of the antenna is maintained even with superstrate. This estab-

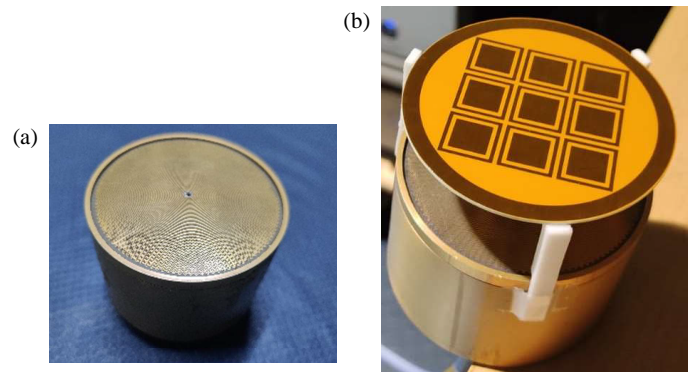


FIGURE 5. Fabricated prototypes. (a) CBAS antenna. (b) CBAS antenna with superstrate.

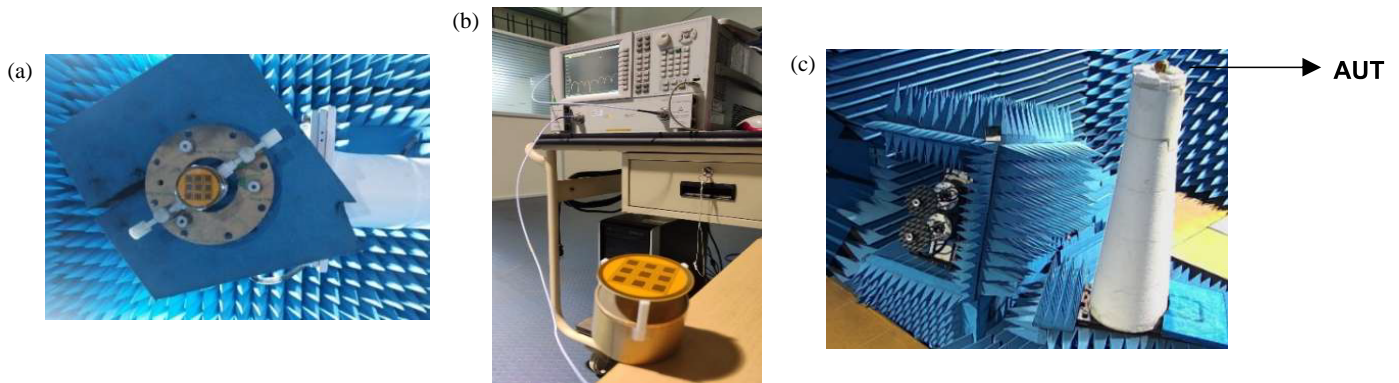


FIGURE 6. Measurement setup for superstrate-based antenna. (a) Radiation pattern. (b) VSWR. (c) RCS.

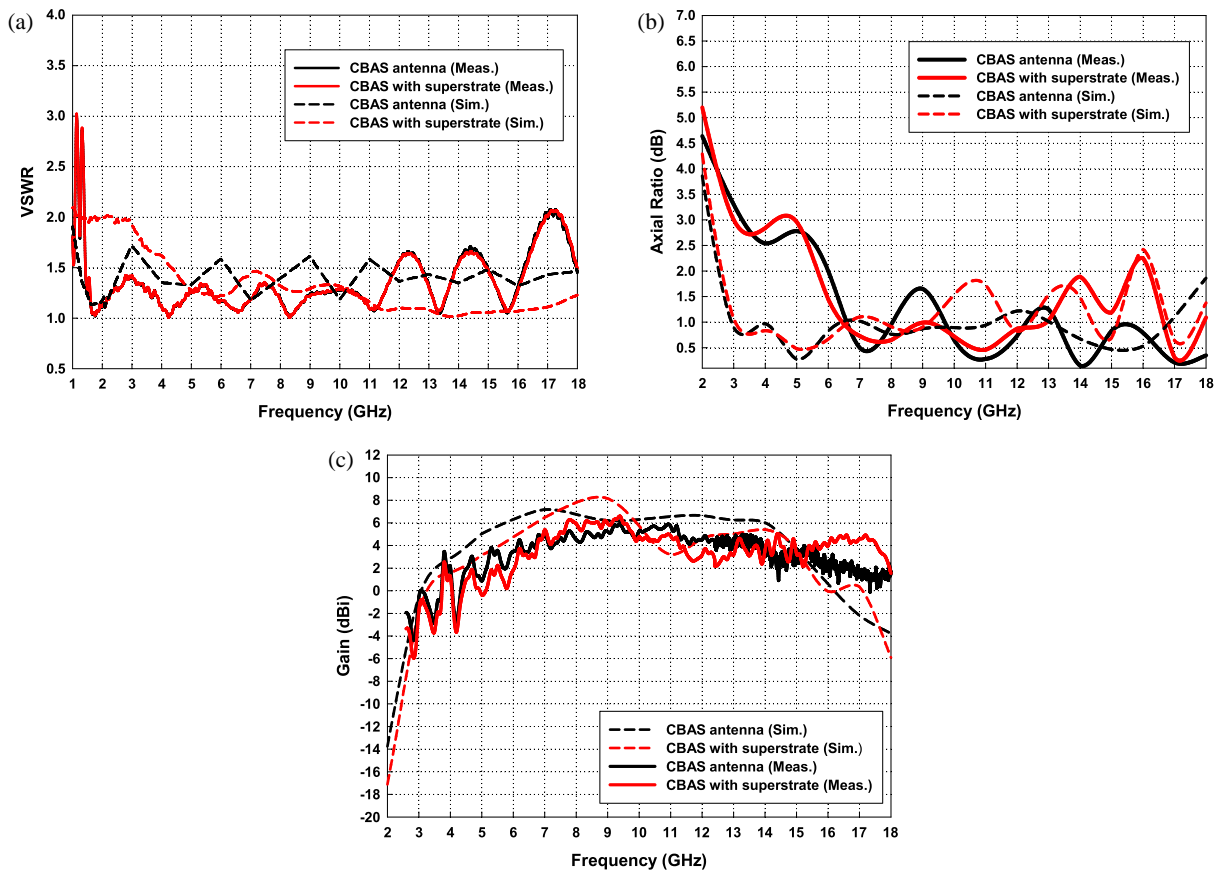


FIGURE 7. EM performance of superstrate-based CBAS antenna. (a) VSWR. (b) Axial Ratio. (c) Gain.

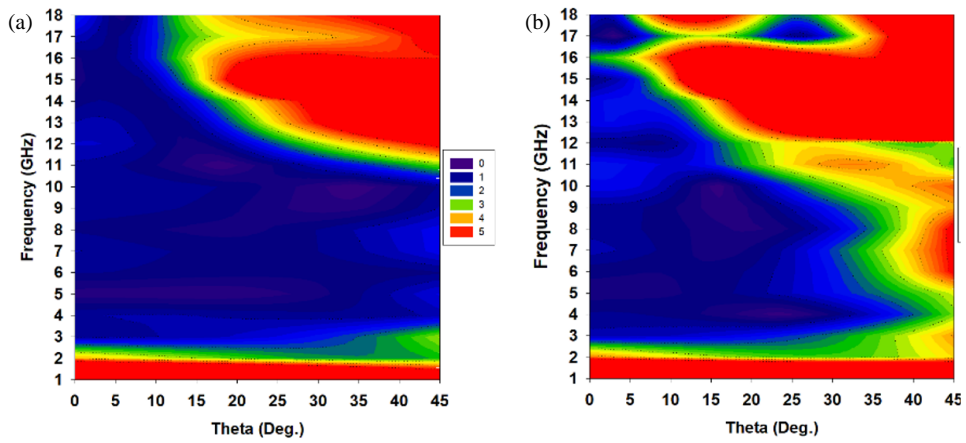


FIGURE 8. Contour plot of axial ratio of CBAS antenna. (a) Antenna alone. (b) Antenna with superstrate.

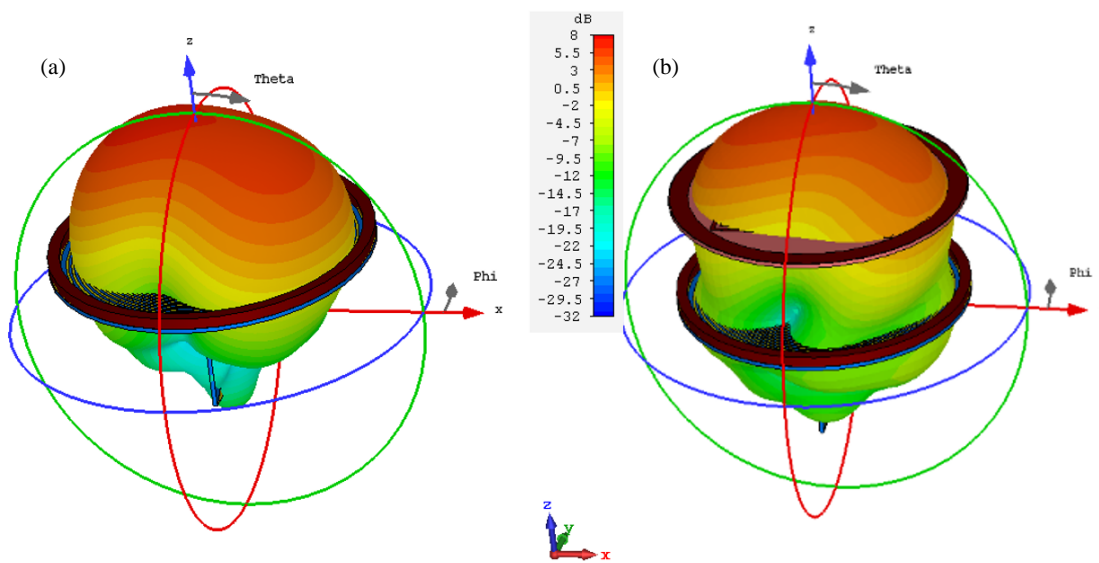


FIGURE 9. Simulated radiation pattern of CBAS antenna at 10 GHz. (a) Antenna alone. (b) Antenna with superstrate.

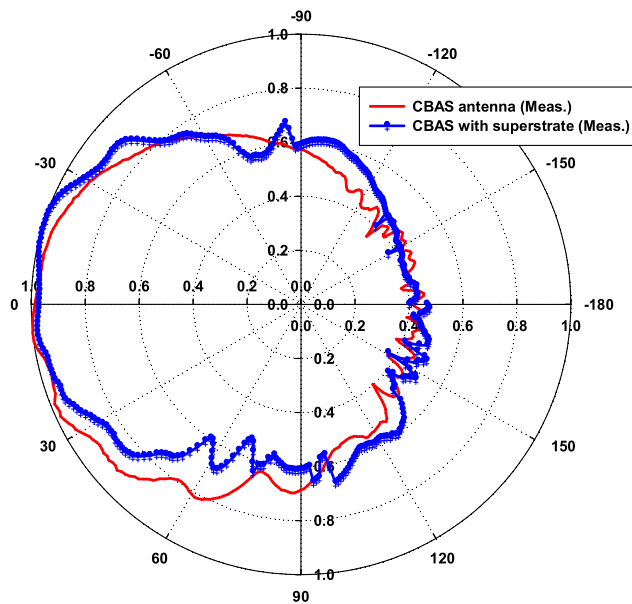


FIGURE 10. Measured radiation pattern of CBAS antenna with superstrate at 10 GHz.

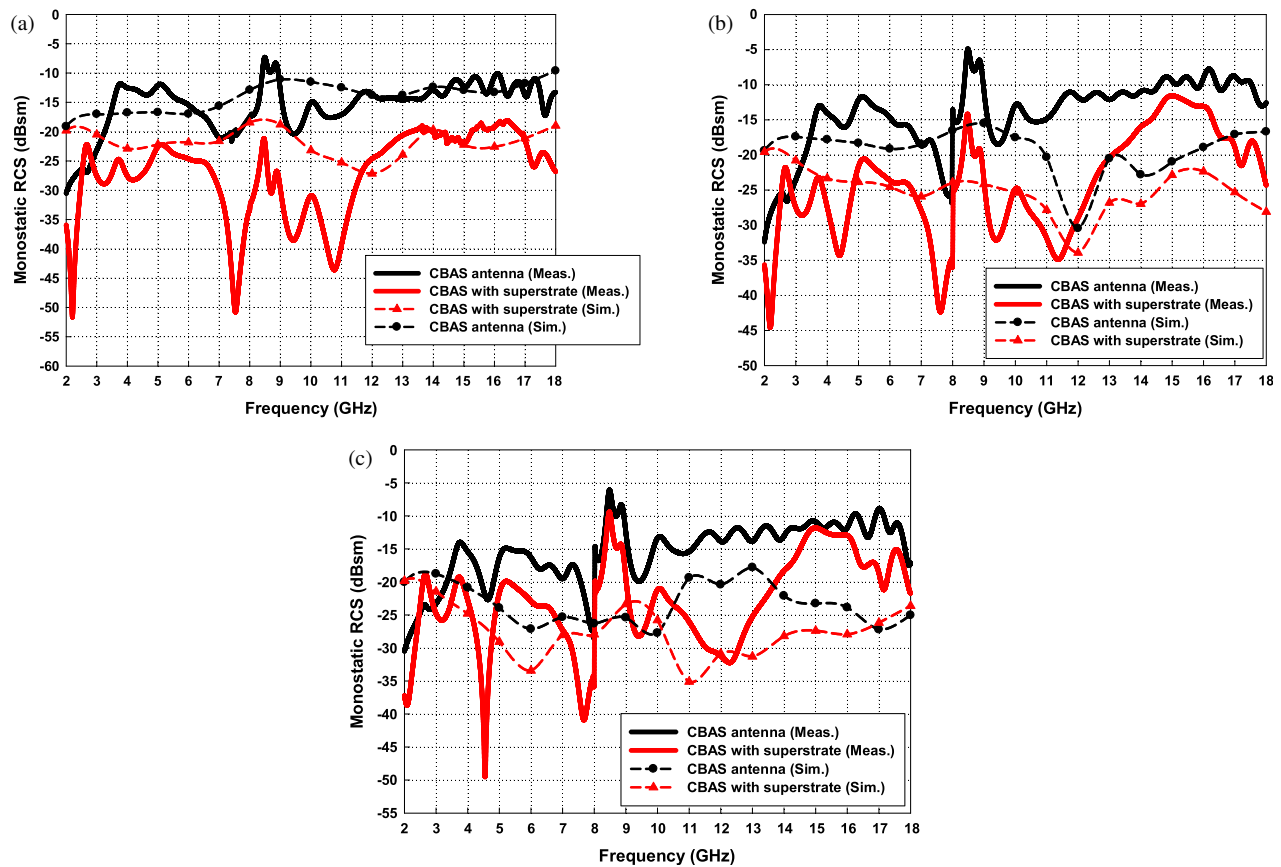


FIGURE 11. Monostatic RCS of CBAS antenna with superstrate. (a) Normal incidence ($\theta = 0^\circ$), (b) $\theta = 10^\circ$, (c) $\theta = 20^\circ$.

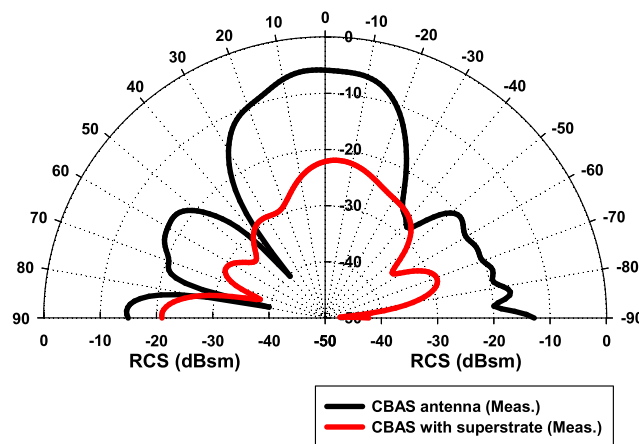


FIGURE 12. Measured monostatic RCS pattern of CBAS antenna with superstrate at 10 GHz.

lishes the efficacy of superstrate-based CBAS antenna w.r.t. the radiation performance.

3.2. Scattering Performance

The measured monostatic RCS at normal incidence for the CBAS antenna with a superstrate has been compared with the simulated results (Fig. 11). Here, the monostatic RCSs for both normal and oblique angles ($\theta = 10^\circ$; $\theta = 20^\circ$) are presented. It is apparent that both simulated and measured results show significant RCS reduction of 6–8 dBsm over the fre-

quency range of 2–18 GHz. The measured monostatic RCS patterns of the CBAS antenna at 10 GHz with and without superstrate are shown in Fig. 12.

Figure 13 presents the contour plot for the bistatic RCS of the CBAS antenna with a superstrate for a normally incident plane wave. The simulated bistatic RCS patterns of the CBAS antenna with and without a superstrate at 9 GHz are shown in Fig. 14. The RCS reduction in the superstrate-based CBAS antenna is very evident in the results. The summary of results is shown in Table 3.

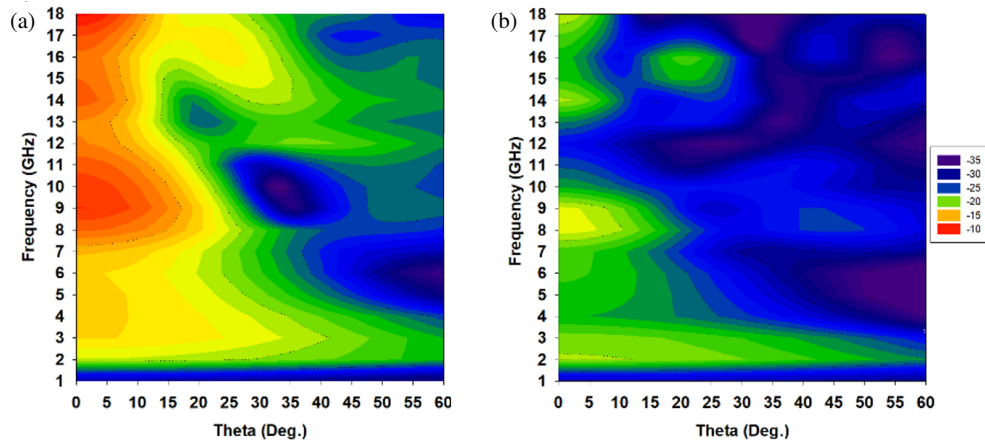


FIGURE 13. Contour plot of simulated bistatic RCS of CBAS antenna with superstrate at normal incidence. (a) CBAS antenna. (b) CBAS antenna with superstrate.

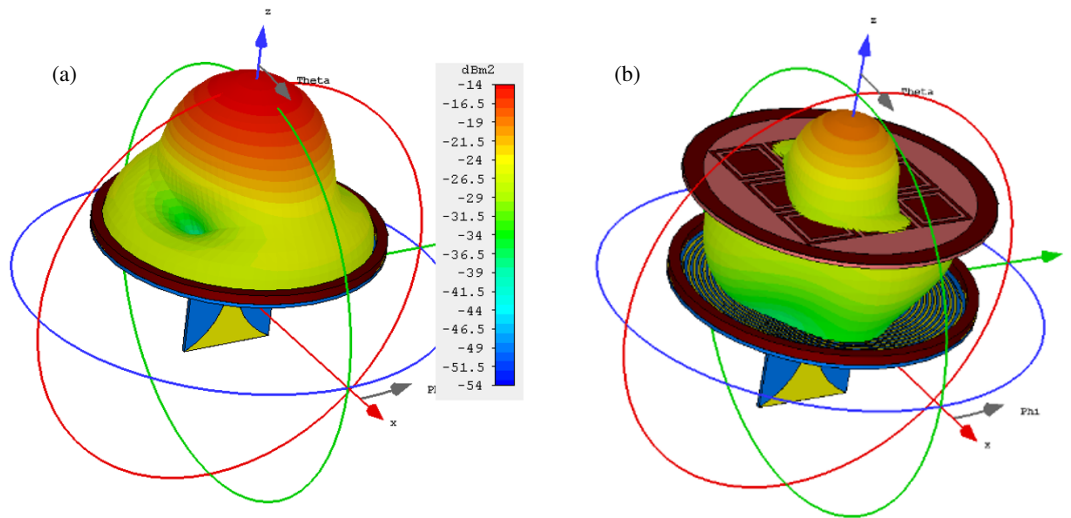


FIGURE 14. Simulated bistatic RCS pattern of CBAS antenna at 9 GHz. (a) Antenna alone. (b) Antenna with superstrate.

TABLE 3. Low RCS superstrate based CBAS antenna (2–18 GHz).

Parameters		CBAS Antenna	Antenna with superstrate	
Radiation Properties	S_{11} (dB)	<-10 dB	<-10 dB	
	VSWR	< 2	<2	
	Maximum Gain (dBi)	7 dBi	8 dBi	
	Axial Ratio (dB)	<3 dB	<3 dB	
Avg. Monostatic RCS reduction (dBsm)	Normal Incidence	-	8 dB	
	Oblique Incidence	$\theta=10^\circ$	-	8 dB
		$\theta=20^\circ$	-	8 dB

4. CONCLUSION

Antennas radiate EM signals for communication, and hence, there is high probability of detection by enemy radars. Therefore, it is imperative to focus on the RCS reduction of these antennas mounted over the aircraft. This paper presents a low-observable superstrate-based cavity-backed Archimedean spiral (CBAS) antenna (2–18 GHz). It is taken care that antenna RCS is reduced without any degradation of its radiation perfor-

mance over the operating frequency range of 2–18 GHz. The superstrate consists of three layers, viz., the resistive patches on the top, dielectric substrate material in the middle, and the bottom metallic pattern. The efficiency of the designed superstrate is established from the fact that the RCS reduction of 8–10 dBsm (on average) has been achieved over 2–18 GHz without any degradation in the radiation performance of the CBAS antenna in terms of VSWR, axial ratio, and gain. Table 3 presents the overall EM and RCS performance of the designed and developed superstrate-based CBAS antenna. It is evident that the developed configuration is a cost-effective solution for low observable, wideband EW antenna (2–18 GHz) with no weight constraints (0.82 mm thick superstrate). It is undoubtedly a preferred candidate for direction finding and RWR antennas for aerospace platforms.

ACKNOWLEDGEMENT

Authors would like to express gratitude to the DRDO-Aeronautical Research & Development Board (AR&DB) for financial support and DSIR-sponsored Common Research

and Technology Development Hub (CRTDH), Dept. of Electronics & Communication Engineering, IIT Roorkee for EM performance and RCS measurements.

REFERENCES

- [1] Zhong, Y.-W., G.-M. Yang, J.-Y. Mo, and L.-R. Zheng, “Compact circularly polarized archimedean spiral antenna for ultrawideband communication applications,” *IEEE Antennas and Wireless Propagation Letters*, Vol. 16, 129–132, 2017.
- [2] Akkaya, E. and F. Güneş, “Ultrawideband, high performance, cavity-backed Archimedean spiral antenna with Phelan balun for direction finding and radar warning receiver applications,” *International Journal of RF and Microwave Computer-Aided Engineering*, Vol. 31, No. 5, e22596, 2021.
- [3] Das, S. K. V., A. Singh, A. A. Gurap, and H. Singh, “Superstrate-based patch antenna array with reduced in-band radar cross section,” *International Journal of Microwave and Wireless Technologies*, Vol. 14, No. 6, 790–802, Jul. 2022.
- [4] Choi, W., Y. H. Cho, C.-S. Pyo, and J.-I. Choi, “A high-gain microstrip patch array antenna using a superstrate layer,” *ETRI Journal*, Vol. 25, No. 5, 407–411, 2003.
- [5] Arora, C., S. S. Pattnaik, and R. N. Baral, “SRR superstrate for gain and bandwidth enhancement of microstrip patch antenna array,” *Progress In Electromagnetics Research B*, Vol. 76, 73–85, 2017.
- [6] Lee, Y. J., W. S. Park, J. Yeo, and R. Mittra, “Directivity enhancement of printed antennas using a class of metamaterial superstrates,” *Electromagnetics*, Vol. 26, No. 3-4, 203–218, 2006.
- [7] Zheng, Y., J. Gao, Y. Zhou, X. Cao, H. Yang, S. Li, and T. Li, “Wideband gain enhancement and RCS reduction of Fabry-Perot resonator antenna with chessboard arranged metamaterial superstrate,” *IEEE Transactions on Antennas and Propagation*, Vol. 66, No. 2, 590–599, 2018.
- [8] Pirhadi, A., H. Bahrami, and J. Nasri, “Wideband high directive aperture coupled microstrip antenna design by using a FSS superstrate layer,” *IEEE Transactions on Antennas and Propagation*, Vol. 60, No. 4, 2101–2106, 2012.
- [9] Ajewole, B., P. Kumar, and T. Afullo, “A microstrip antenna using I-shaped metamaterial superstrate with enhanced gain for multiband wireless systems,” *Micromachines*, Vol. 14, No. 2, 412, 2023.
- [10] Gao, X., Y. Zhang, and S. Li, “High refractive index metamaterial superstrate for microstrip patch antenna performance improvement,” *Frontiers in Physics*, Vol. 8, 580185, Sep. 2020.
- [11] Liu, Y., Z. Liu, Q. Wang, and Y. Jia, “Low-RCS antenna array with switchable scattering patterns employing microfluidic liquid metal alloy-based metasurface,” *IEEE Transactions on Antennas and Propagation*, Vol. 69, No. 12, 8955–8960, Dec. 2021.
- [12] Wang, F., Y. Wang, X. Zhang, L. Liu, K. Li, and Y. Ren, “Wideband low-RCS and gain-enhanced antenna using frequency selective absorber based on patterned graphene,” *Scientific Reports*, Vol. 14, 9306, 2024.
- [13] Zhang, C., X.-Y. Cao, J. Gao, and S.-J. Li, “Wideband high-gain and low scattering antenna using shared-aperture metamaterial superstrate,” *Radioengineering*, Vol. 27, No. 2, 379–385, Jun. 2018.
- [14] Gonçalves Machado, G., R. Cahill, V. Fusco, and G. Conway, “Frequency selective superstrate absorber for wideband RCS reduction of metal-backed antennas,” *IET Microwaves, Antennas & Propagation*, Vol. 15, No. 4, 441–450, 2021.